3-Leg Full-Bridge Resonant Inverter for Different Material Vessel Induction Cooking Application

Dr. P. Sharath Kumar*[1], Ch. Sai Charan*[2], K. Dileep Kumar*[3], G. Shiva Prakash Reddy*[4],
G. Revanth*[5], Dr. S. Ravichandran*[6]

** Department of Electrical & Electronics Engineering, Sreenidhi Institute of Science and Technology,
Yamnampet, Ghatkesar, Hyderabad, Telangana, INDIA*

ABSTRACT
This paper presents a 3-leg full-bridge resonant inverter configuration for different material vessel induction cooking application. The proposed 3-leg full-bridge resonant inverter configuration features simultaneous heating of three different material vessels, and independent output power control of each load. In this proposed configuration, three different induction heating loads are simultaneously operated at their 1.05 times of respective resonant frequencies to achieve ZVS. Iron, steel, and aluminum material vessels are used as induction loads. The output powers are independently controlled by using an asymmetric duty cycle control technique. The proposed 3-leg full-bridge resonant inverter configuration is designed and simulated in MATLAB / Simulink.
Keywords - *Full-bridge resonant inverter configuration, Induction cooking, Multiple load, Asymmetric duty cycle control, ZVS*

I.   INTRODUCTION

Now a days utilization of electrical energy is a basic necessity of human life for wide use of electrical appliances. Induction heating has several applications. Induction heating operates on high frequency AC supply. Induction cooking is one of the main applications of induction heating. Recent times have shown development of semiconductor devices and research in high frequency inverter circuits. There is progress in new control schemes and circuit modifications by the use of power semiconductor devices such as MOSFETs, IGBTs, MCTs and SITs having high efficiency and high reliability. The power semiconductor devices offer reduced switching losses by using soft switching techniques at high frequency operation. Induction heating method is a far better approach than other conventional methods because of generation of magnetic flux to inducing eddy currents in load based on Faraday's law of electromagnetic induction principle and there by producing heat by Joules heating principle [1]. In conventional methods the heat is transferred from heat source to load by conduction or radiation. But in induction heating method the heat is developed inside the load due to generation of eddy currents. The heat generated by eddy currents in the heating load is concentrated in a peripheral layer at skin depth (δ) [2], which is explained by

$$\delta = \sqrt{\frac{\rho}{\pi \mu f}} = \sqrt{\frac{1}{4\pi^2 \times 10^{-7}}} \times \sqrt{\frac{\rho}{\mu_r f}} \qquad (1)$$

where, ρ is electrical resistivity, μ is magnetic permeability and μ_r is relative magnetic permeability of the load material and f is switching frequency of the inverter circuit.

Generally using topologies in induction cooking application are quasi resonant inverter, half bridge inverter and full bridge inverter. Full bridge inverter supplies a peak to peak voltage across the load which is twice the source voltage. So it leads to high power transfer to load from the source. Full bridge inverter has become very popular over other topologies and is widely used in high power applications [2].

Full bridge resonant inverter is generally used to energize the induction heating coil with high frequency current to generate high frequency magnetic flux between the induction heating coil and the cooking vessel. Consequently, high frequency eddy current is induced at a peripheral layer of skin depth level, inside the vessel and finally heat is developed in the bottom area of the vessel. The full bridge inverter takes the energy from the input source and converting into the dc voltage by diode rectifier. This dc supply is fed to inverter and converts into a high frequency ac voltage, supplying a high frequency current to the induction heating coil. The general series resonant inverter circuit for induction cooking application is shown in Fig. 1.
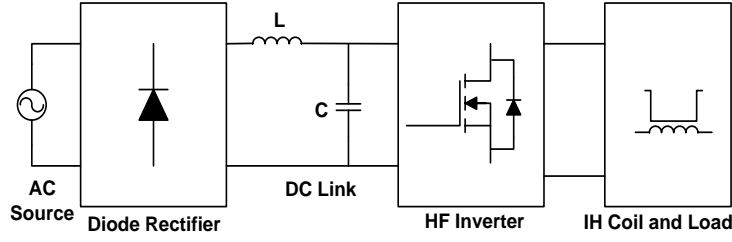
Fig. 1. Typical circuit of high frequency induction cooking application

Induction cooking applications use Variable Frequency scheme, Pulse Frequency Modulation (PFM), Pulse Amplitude Modulation (PAM), and Phase Shift Modulation (PSM) to control the output power. In Variable Frequency scheme for constant load to control output power, varying the normalized switching frequency. In case of below resonance operation, filter components are large for the low-frequency range. In PAM control for constant load amplitude of the source voltage is varied to control the output power. In PFM control the resonant frequency is tracking, when load changes by using PLL circuit. PFM control has ZVS soft switching operating region is relatively narrow. PSM control gives high efficiency at higher duty ratio [3]-[4]. To overcome these problems, PWM technique is used.

This paper proposes full bridge resonant inverter configuration with two parallel loads for induction cooking application. The characteristics of full bridge series resonant inverter and proposed output power control scheme are explained in detail. In this configuration, synchronization of load switch switching pulse with inverter output voltage used for control the output power of each load independently. This configuration can be extended to multiple loads.

II.   FULL-BRIDGE SERIES RESONANT INVERTER

A high frequency full bridge series resonant inverter is used to energize the IH coil. It generates high frequency magnetic flux and linking with the load. Consequently high frequency eddy current induces at skin depth level in the vessel bottom area. Finally heat is developed inside the vessel due to eddy currents. The full bridge series resonant inverter for induction cooking application is shown in Fig. 2.
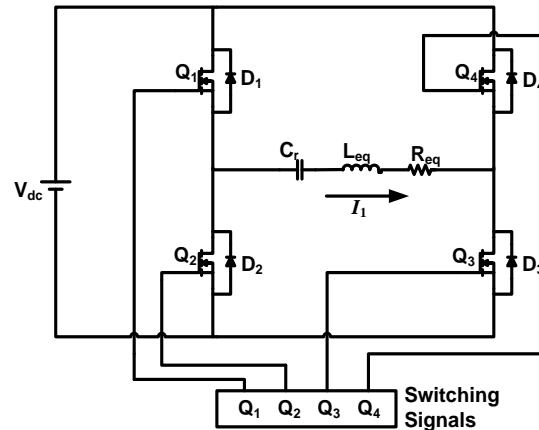

Fig. 2. Full bridge resonant inverter for IH cooking application

A. Operating Principle of Induction Heating

Operating principle of IH is that when induction heating coil is energized by high frequency current, it produces magnetic flux. It causes eddy currents that occur in heating load and this result in heating effect. The induced eddy currents are concentrated in the vessel bottom layer at skin depth (δ) level [2]. The load surface resistance (R_L) is determined by the load skin depth and its material specific resistance is shown in below expression,

$$R_L = \frac{\rho}{\delta} = k\sqrt{\rho\mu_r f_s} \tag{2}$$

where *k* is constant = 0.00198692

The load parameters depends on several variables including the shape of the heating coil, the spacing between the heating coil and cooking vessel (load), their electrical conductivity and magnetic permeability, and the inverter switching frequency.

B. Equivalent Circuit of IH Coil and Load

A linear equivalent model of the IH coil and load represented by the effective equivalent inductance (L_{eq}) in series with effective equivalent resistance (R_{eq}) is referred to the input side of IH coil.
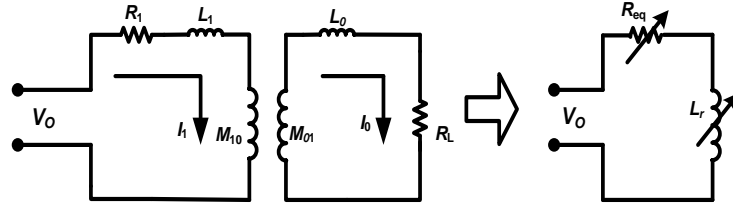
Fig. 3. Equivalent circuit of IH coil with load

Fig. 3, shows the equivalent circuits for IH coil with load parameters. Load parameters are taken as single turn short circuited secondary winding.

The circuit elements are represented as:
1) R_L surface resistance of the load
2) L_0 inductance of the load
3) R_1 resistance of IH coil
4) L_1 inductance of IH coil
5) I_0, I_1 Load current and IH coil current
6) M_{10}, M_{01} the mutual inductance between IH coil and load.

The voltage equations for the above equivalent circuit:

$$V_0 = I_1 R_1 + L_1 \frac{dI_1}{dt} + M_{10} \frac{dI_0}{dt} \tag{3}$$

$$0 = I_0 R_L + L_0 \frac{dI_0}{dt} + M_{01} \frac{dI_1}{dt} \tag{4}$$

From (3) and (4) equations,

$$R_{eq} = R_1 + \frac{(\omega M)^2 . R_L}{R_L{}^2 + (\omega L_0)^2} \tag{5}$$

$$L_r = \left\{ L_1 - \frac{(\omega M)^2 . L_0}{R_L{}^2 + (\omega L_0)^2} \right\} \tag{6}$$

$$R_{eq} = R_1 + A^2 R_L \tag{7}$$

$$L_r = \{ L_1 - A^2 L_0 \} \tag{8}$$

where, $M_{10} = M_{01} = M$

and $\quad A = \dfrac{(\omega M)}{\sqrt{R_L{}^2 + (\omega L_0)^2}} = \dfrac{M}{L_0} \;\; at \;\; \omega L_0 \gg R_L$

C. Characteristics of resonant tank

The resonant tank circuit in class-D/E inverter shown in Fig. 3 can be described by the following parameters:

The resonant angular frequency is

$$\omega_r = \frac{1}{\sqrt{L_r C_r}} \tag{9}$$

The normalized switching frequency is

$$\omega_n = \frac{\omega_s}{\omega_r} \tag{10}$$

where ω_s = switching angular frequency = $2\pi \times f_s$
$\qquad f_s$ = switching frequency

The characteristic impedance is

$$Z_0 = \sqrt{\frac{L_r}{C_r}} = \frac{1}{\omega_r C_r} = \omega_r L_r \tag{11}$$

The IH load quality factor is

$$Q = \frac{\omega_r L_r}{R_{eq}} = \frac{1}{\omega_r C_r R_{eq}} = \frac{Z_0}{R_{eq}} \tag{12}$$

The resonant tank circuit impedance is given by

$$Z_{eq} = R_{eq} + j \left(\omega_s L_r - \frac{1}{\omega_s C_r} \right) \tag{13}$$

$$= R_{eq} \left(1 + jQ \left(\omega_n - \frac{1}{\omega_n} \right) \right) \tag{14}$$

$$|Z_{eq}| = R_{eq} \sqrt{1 - Q^2 \left(\omega_n - \frac{1}{\omega_n} \right)^2} \tag{15}$$

The phase angle between output voltage and current is

$$\emptyset = \tan^{-1}\left(Q\left(\omega_n - \frac{1}{\omega_n}\right)\right) \tag{16}$$

The voltage across the resonant tank circuit V_d is

$$V_d = \begin{cases} V_{dc}, & for\ 0 < \omega_s t \leq \pi \\ -V_{dc}, & for\ \pi < \omega_s t \leq 2\pi \end{cases} \tag{17}$$

The fundamental component of V_d can be found from Fourier analysis,

$$V_d(\omega) = V_m \sin \omega_s t,\ for\ 0 < \omega_s t \leq \pi \tag{18}$$

where

$$V_m = \frac{4}{\pi} V_{dc} \approx 1.273\ V_{dc} \tag{19}$$

The load current through the series resonant tank circuit is derived by

$$I_1 = I_m \sin(\omega_s t - \emptyset) \tag{20}$$

where

$$\begin{aligned} I_m &= \frac{V_m}{|Z_{eq}|} = \frac{4V_{dc}}{\pi|Z_{eq}|} \\ &= \frac{4V_{dc}\cos\emptyset}{\pi R_{eq}} \\ &= \frac{4V_{dc}}{\pi R_{eq}\sqrt{1 + Q^2\left(f_n - \frac{1}{f_n}\right)^2}} \end{aligned} \tag{21}$$

The output power can be derived as following by using eq. (21)

$$\begin{aligned} P_{out} &= \frac{I_m^2}{2} R_{eq} \\ &= \frac{8V_{dc}^2 \cos\emptyset^2}{\pi^2 R_{eq}} \\ &= \frac{8V_{dc}^2}{\pi^2 R_{eq}\left(1 + Q^2\left(f_n - \frac{1}{f_n}\right)^2\right)} \end{aligned} \tag{22}$$

From the eq. (22) the output power can be controlled by varying the load current by the duty ratio of the inverter. The output power also depends on load quality factor and normalized switching frequency. The inverter operates at switching frequency above its resonant frequency to ensure inverter switching devices are operating in ZVS region.

III. PROPOSED 3-LEG FULL-BRIDGE RESONANT INVERTER CONFIGURATION

The output power of multiple loads are individually controlled is the main aim in full bridge series resonant inverter [5]. We propose a 3-leg full bridge series resonant inverter configuration with different material vessels and independent output power control achieved by asymmetric duty cycle control technique. The 3-leg full bridge series resonant inverter operates at three different switching frequencies of each leg are 30kHz, 150kHz, and 450kHz respectively. The inverter switching frequency is chosen above their resonant frequency of 1.05 times for ZVS operation of inverter switching devices.

One leg of the inverter is switched at low frequency (LF) and the second leg of the inverter is switched at medium frequency (MF) and the other leg is switched at high frequency (HF). They are marked as LF leg, MF leg, and HF leg respectively. ADC control technique is used with each leg. Resonant frequencies of load-1, load-2 and load-3 are $f_{rl} = \frac{1}{2\pi\sqrt{L_{r1}C_{r1}}}$, $f_{rm} = \frac{1}{2\pi\sqrt{L_{r2}C_{r2}}}$, and $f_{rh} = \frac{1}{2\pi\sqrt{L_{r3}C_{r3}}}$ respectively. Controlling the output power of each load is done individually, with asymmetric duty cycle control technique. This configuration can be extended to multiple loads.
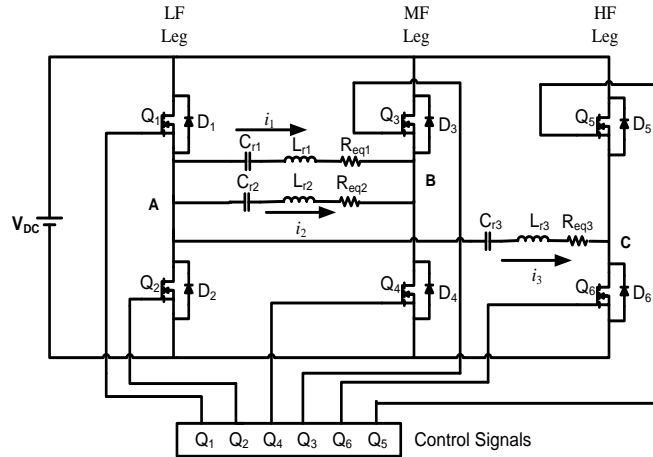
Fig. 6. Proposed 3-leg full bridge series resonant inverter configuration

IV.   SIMULATION AND RESULTS

To verify theoretical predictions of proposed 3-leg full bridge series resonant inverter configuration simulated in MATLAB/Simulink. ZVS operation for inverter switching devices is achieved by choosing the switching frequency more than its resonant frequency. The proposed inverter configuration is simulated with the parameters as shown in Table I.

TABLE I
Parameters of 3-leg series resonant inverter configuration

Item	Symbol	Value
Source voltage	V_{DC}	50V
Equivalent resistance of load-1	R_{eq1}	1.95Ω
Equivalent inductance of load-1	L_{r1}	68μH
Equivalent resistance of load-2	R_{eq2}	2.6Ω
Equivalent inductance of load-2	L_{r2}	68μH
Equivalent resistance of load-3	R_{eq3}	3.6Ω
Equivalent inductance of load-3	L_{r3}	50.7μH
Resonant capacitor of load-1	C_{r1}	0.44μF
Resonant capacitor of load-2	C_{r2}	0.02μF
Resonant capacitor of load-3	C_{r3}	2.7nF
Low resonant frequency	f_{rl}	29.07kHz
Medium resonant frequency	f_{rm}	142.41kHz
High resonant frequency	f_{rh}	430.16kHz
Low Switching Frequency	f_l	30kHz
Medium Switching Frequency	f_m	150kHz
High Switching Frequency	f_h	450kHz

Fig. 7, shows the admittance curves of different material of induction heating resonant loads. From these characteristics, each load can be allowed only respective frequency current only. In general, the duty ratio is defined as
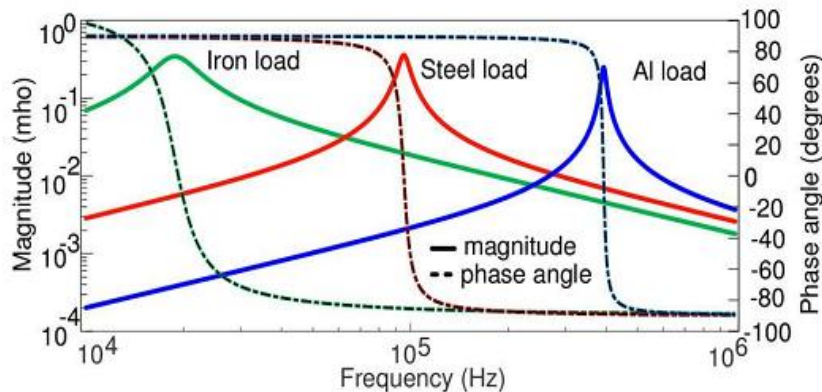
Duty ratio (D) $= \dfrac{T_{on}}{T/2}$

Fig. 7. Admittance curves of different induction heating resonant loads
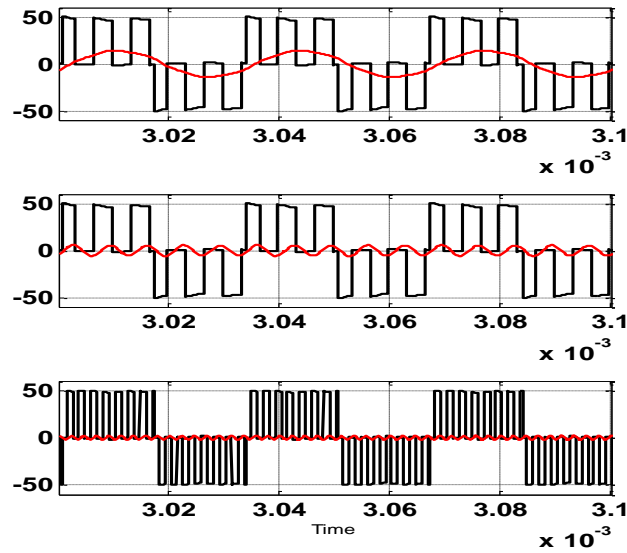
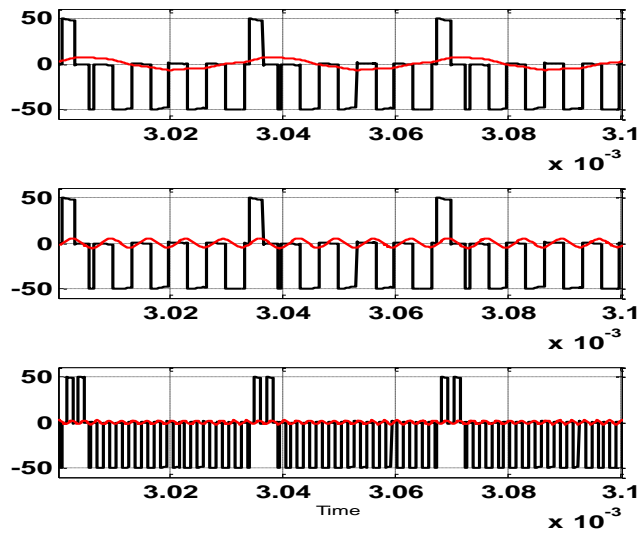Fig. 8. Simulation results for $D_l=1$, $D_m=1$, $D_h=1$

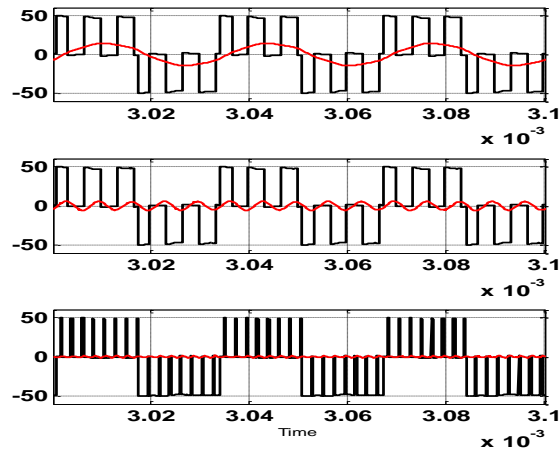Fig. 9. Simulation results for $D_l=0.3$, $D_m=1$, $D_h=1$

Fig. 10. Simulation results for $D_l=1$, $D_m=1$, $D_h=0.3$

Table-II
Current magnitudes with different duty-ratios

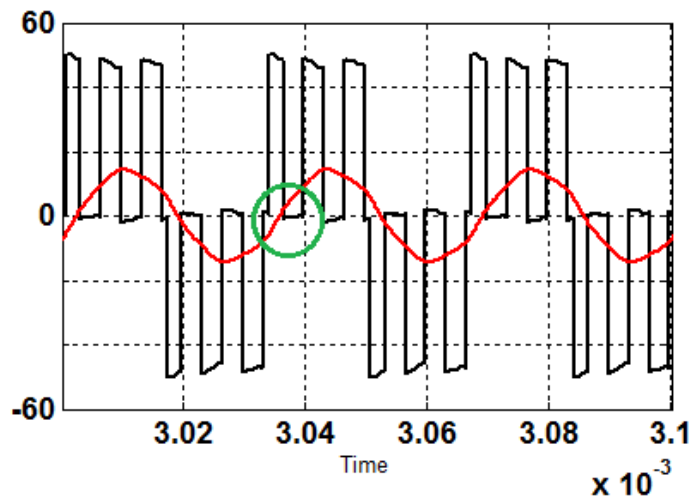| D_l	D_m	D_h	Simulation (Load currents in Amps)		
			I_{lf} (rms)	I_{mf} (rms)	I_{hf} (rms)
1	1	1	10.11	4.1	1.62
0.6	1	1	7.92	4.1	1.62
0.3	1	1	5.16	4.1	1.62
1	0.6	1	10.11	3.18	1.62
1	0.3	1	10.11	1.69	1.62
1	1	0.6	10.11	4.1	1.34
1	1	0.3	10.11	4.1	0.85

Fig. 8. ZVS at LF leg for D_l=1, D_m=1, D_h=1

Current magnitudes of each load at different duty-ratios are tabulated in Table-2. From the above table, it is observed that the each load currents are controlled independently with respective inverter leg duty-ratios.

In Figs. 4.11(b) and 4.11(c), it can be observed that for certain cycles, ZVS for leading leg devices only is possible. During this zone, ZVS for lagging leg devices is not possible and vice-versa. Hence ZVS is not ensured in every cycle for both leading and lagging leg devices of MF and HF legs of inverter. ZVS operation of LF leg of inverter is not significant due to low switching frequency and hence low switching losses. In MF and HF legs of inverter there is difficulty in achieving ZVS for both legs simultaneously in every cycle.

V. CONCLUSIONS

In this paper, a multi-load 3-leg full-bridge resonant inverter topology is proposed for different material vessel IH loads. The inverter first leg is operated at low frequency and second leg is operated at medium frequency of 30kHz, and 150kHz suitable for iron and steel vessels. The third leg is operated at high frequency of 450 kHz suitable for aluminum vessel. Independent power control is achieved using asymmetric duty cycle control. The proposed inverter topology is designed, simulated in MATLAB / Simulink. This topology provides advantages of compatibility with ferromagnetic and non-ferromagnetic material vessels, independent load power control with ZVS operation.
.

REFERENCES

[1] W. C. Moreland, "The induction range: Its performance and its development problems," *IEEE Trans. Industry Applications*, vol. IA-9, no. 1, 1973, pp. 81–85.
[2] Masaki Miyamae, Takahiro Ito, Kouki Matsuse, Masayoshi Tsukahara, "Performance of a High Frequency Quasi-Resonant Inverter with Variable-Frequency Output for Induction Heating", *IEEE 7th International Power Electronics and Motion Control Conference*, Harbin, China, 2012.
[3] Mokhtar Kamli, Shigehiro Yamamoto, and Minoru Abe, "A 50-150 kHz Half-Bridge Inverter for Induction Heating Applications," *IEEE Trans. Industrial Electronics*, vol. 43, no.1, 1996, pp. 163–172.

[4]   S.M.W. Ahmed, M.M. Eissa, M. Edress, T.S. Abdel-Hameed, , "Experimental investigation of full bridge Series Resonant Inverters for Induction-Heating Cooking Appliances", *4th IEEE Conference on Industrial Electronics and Applications, ICIEA 2009*, pp.3327-3332..

[5]   Atsushi Okuno, Hitoshi Kawano, Junming Sun, Manabu Kurokawa, Akira Kojina, Mutsuo Nakaoka, "Feasible Development of Soft-Switched SIT Inverter with Load-Adaptive Frequency-Tracking Control Scheme for Induction Heating," *IEEE Trans. Industry Applications*, vol. 34, no. 4, 1998, pp. 713 - 718.

[6]   Young-Sup Kwon, Sang-Bong Yoo, Dong-Seok Hyun, "Half-Bridge Series Resonant Inverter for Induction Heating Applications with Load-Adaptive PFM Control Strategy", *14th Applied Power Electronics Conference and Exposition, APEC' 99*, vol. 1, 1999, pp. 575 - 581.

[7]   L. Grajales, J. A. Sabate, K. R. Wang, W. A. Tabisz, F. C. Lee, "Design of a 10 kW, 500 kHz Phase-Shift Controlled Series-Resonant Inverter for Induction Heating", *Industry Applications Society Annual Meeting*, vol. 2, 1993,   pp. 843-849.

[8]   Satoshi Nagai, Hirokazu Nagura, Mutsuo Nakaoka, Atsushi Okuno, "High-Frequency Inverter with Phase-Shifted PWM and Load-Adaptive PFM Control Strategy for Industrial Induction-Heating", *Industry Applications Society Annual Meeting*, vol. 3, 1993, pp. 2165-2172.

[9]   Jinfei Shen, Hongbin Ma,Wenxu Yan, Jing Hui, Lei Wu, "PDM and PSM Hybrid Power Control of a Series-Resonant Inverter for Induction Heating Applications", *IEEE Conference on Industrial Electronics and Applications*, ICIEA 2006.

[10]   J. M. Burdio, L. A. Barragan, F. Monterde, D. Navarro, J. Acero, "Asymmetrical voltage-   cancellation control for full-bridge series   resonant inverters," *IEEE Trans. Power Electronics*, vol. 19, no. 2, 2004, pp. 461-469.

[11]   Hector Sarnago, Oscar Lucia, Arturo Mediano, J.M. Burdio, "Class D/DE Dual-Mode Operation Resonant Converter for Improved-Efficiency Domestic Induction Heating System," *IEEE Trans. Power Electronics*, vol. 28, no. 3, March 2013, pp. 1274-1285.

[12]   F. Forest, E. Laboure, F. Costa, J.Y. Gaspard, "Principle of a multi-load / single converter system for low power induction heating," *IEEE Trans. Power Electronics*, vol.15, no. 2, 2000, pp. 223 - 230.

[13]   Jose M. Burdio, Fernando Monterde, Jose R. Garcia, Luis A. Barragan, Abelardo Martinez, "A Two-Output Series-Resonant Inverter for Induction-Heating Cooking Appliances," *IEEE Trans. Power Electronics*, vol. 20, no. 4, 2005, pp. 815 - 822.

[14]   S. Zenitani, M. Okamoto, E. Hiraki, T. Tanaka, "A Charge Boost Type Multi Output Full Bridge High Frequency Soft Switching Inverter for IH Cooking Appliance," *14th International Power Electronics and Motion Control Conference (EPE-PEMC)*, 2010, pp. T2-127 - T2-133.

[15]   Oscar Lucia, J.M. Burdio, I. Millan, J. Acero, D. Puyal, "Load-Adaptive Control Algorithm of Half-Bridge Series Resonant Inverter for Domestic Induction Heating," *IEEE Trans. Industrial Electronics*, vol.56, no. 8, August 2009, pp. 3106-3116.

[16]   Oscar Lucia, Jose M. Burdio, Luis A. Barragan, Claudio Carretero, Jesus Acero, "Series Resonant Multi-inverter with Discontinuous-Mode Control for Improved Light-Load Operation," *IEEE Trans. Industrial Electronics*, vol. 58, no. 11, November 2011, pp. 5163-5171.

[17]   Oscar Lucia, I. Urriza, Luis A. Barragan, D. Navarro, Oscar Jimenez, J.M.Burdio, "Real Time FPGA-Based Hardware in the Loop Simulation Test Bench Applied to Multiple Output Power Converters," *IEEE Trans. Industry Applications*, vol. 47, no. 2, March/April 2011, pp. 853-860.

[18]   Oscar Lucia, Claudio Carretero, J.M. Burdio, Jesus Acero, and Fernando Almazan, "Multiple-Output Resonant Matrix Converter for Multiple Induction Heaters," *IEEE Trans. Industry Applications*, vol.48, no. 4, July/August 2012, pp. 1387-1396.